Studies of a Tripodal Biomimetic Siderophore Analog: An Efficient Encapsulation for Fe(III) Ion

Baral, Minati**+; Kaur, Kirandeep

Department of Chemistry, National Institute of Technology, Kurukshetra-136119, Haryana, INDIA

Kanungo, B.K.

Department of Chemistry, Sant Longowal Institute of Engineering & Technology, Longowal, Punjab-148106, INDIA

ABSTRACT: *A new tris-(2-aminoethyl)amine (TREN) capped tripodal Schiff base ligand has been developed by mimicking structural features of a natural siderophore, Bacillibactin, by substituting the catechol units with salicylaldehyde and employing amino acid as spacer. Synthesis of the ligand N-[2-[bis[2-[[2-[(2-hydroxyphenyl)methylamino]acetyl] amino]ethyl]amino]ethyl]-2-[(2-hydroxyphenyl)methylamino]acetamide(TRENglySAL) includes condensation of salicylaldehyde and amino acid (glycine) followed by an in-situ reduction of the produced Schiff base, followed by further condensation with TREN. The complexation behavior of the ligand with Fe(III) has been investigated by potentiometric and UV-Vis spectrophotometric method at temperature 25 ±1°C and 0.1 M ionic strength. Seven protonation constants were obtained of the ligand: three each for secondary amine and phenolic protons and one for tertiary nitrogen of capping TREN moiety. The formation constants (log β_{11n}) of different complex species MLH_3, MLH_2, MLH, ML and MLH_{-1} are found to be 35.15, 32.09, 27.91, 25.32 and 17.32 respectively. These results indicate that the ligand is an excellent iron binding chelator. Significant electronic spectral variations during complex formation at higher pH also provide a scope for the ligand to act as an optical pH sensor towards Fe (III) metal ion in biological systems. Structures of the ligand and metal complexes are proposed through experimental findings along with the theoretical semi-empirical PM3 calculation. The theoretical spectroscopic results are found to be comparable with the experimental finding.*

KEYWORDS: *Siderophores; Bacillibactin; TREN; Biomimetic synthesis; Protonation constants; Stability constants.*

INTRODUCTION

Iron, in its trivalent state, has low availability in bio-system due to its low solubility (pK_S=38) at neutral pH [1]. However, its solubility can be increased by binding with siderophores. Siderophores, naturally occurring low molecular weight compounds, are produced by certain microorganisms. They form soluble complexes with iron[2]. Two important siderophores are enterobactin [3-5] and Bacillibactin [11]. They contain L-serine and

** To whom correspondence should be addressed.*

+ E-mail: minatibnitkkr@gmail.com

1021-9986/2020/3/241-256 16/$/6.06

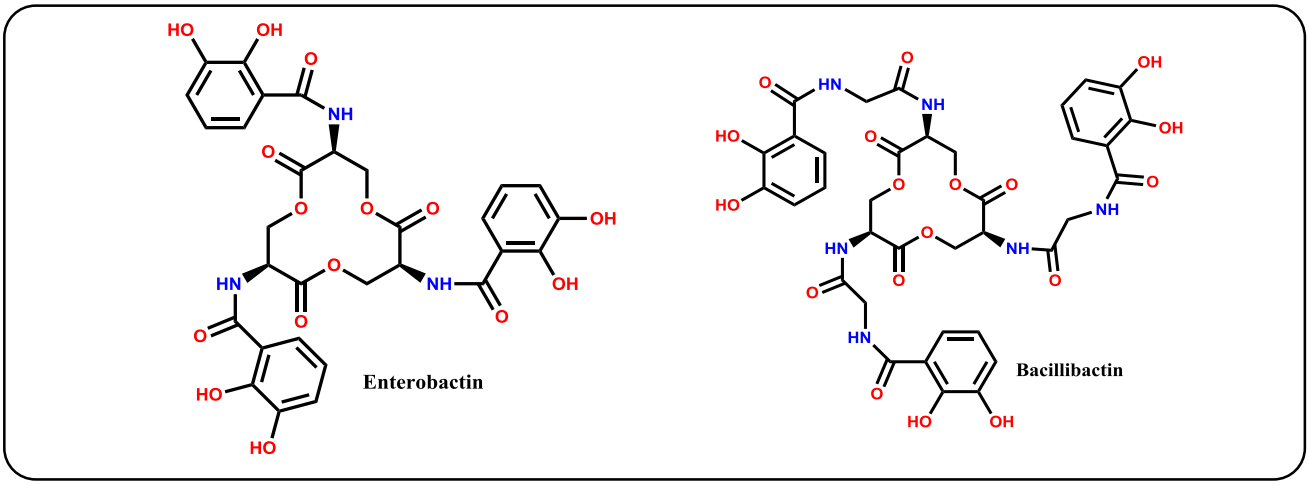

Fig. 1: The molecular structure of Enterobactin and Bacillibactin.

L-threonine as central units (Fig. 1) respectively and comprise 2, 3-catechol as a binding unit. They exhibit very high ferric complex formation constants (K_f) at neutral pH (10^{49} for Enterobactin and 10^{48} for Bacillibactin) forming hexacoordinated complexes with six catecholate oxygen donors. Research findings show that a large number of factors are responsible for the stability of the metal complexes like ligand basicity, structural pre-organization or predisposition and intrinsic basicity of donor atoms. In Bacillibactin, an amino acid spacer separates the trilactone backbone from the catecholamide arms allows extra flexibility and favors formation of the stable complex. It is difficult to pinpoint the effect of the individual components of the siderophores towards the stability of the iron complex only by analyzing the structure of natural siderophores. Mimicking naturally occurring siderophores, however, can provide a way in identifying the key structural features to highlight their contribution towards the overall stability of the ferric complex

Some structural analogs of the natural siderophores [6-10] are synthesized in which one or more components of the siderophores are altered with some structurally similar component, and, their effect has been judged by analyzing the formation constants. Study of TRENGlyCAM, an analog of Bacillibactin (pM =30.9 at pH =7.4), shows the effect of amino acid spacer on the overall stability of the complexes in comparison to complexes of enterobactin analog, TRENCAM (pM =27.8 at pH =7.40 [11]. The trilactone backbone of enterobactin and bacillibactin appears to be perfect for the size of the ferric ion, while TREN caps as a slightly smaller than optimal. The size deficiency is compensated by the addition of the amino acid spacer for TREN based ligands allowing for higher stable complexes. Such architecture of ligand framework leads to pre-organization of the structure in a way where metal ion gets encapsulated to form thermodynamically stable octahedral complex [12]; the stability may be comparable to that of naturally occurring siderophores and even more than that of EDTA and DTPA with Fe(III) [13].

Keeping in view of the importance of the analogs of natural siderophores, a new synthetic analog of bacillibactin with some structural variations, TRENglySAL(Fig. 2), is reported in this communication, wherein tris-(2-aminoethyl) amine (TREN) as the central unit, salicylaldehyde as the binding moiety and glycine as the spacer unit are incorporated. Complexation behavior of the ligand towards Fe(III) is evaluated by potentiometrically, spectrophotometrically and theoretical studies. Protonation constants and formation constants were determined, and formation of various complex species are suggested. The possible geometries of the metal complexes are proposed based on experimental and computational findings.

EXPERIMENTAL SECTION

Materials and Measurements

All the chemicals and solvents used were of analytical grade and available commercially. Glycine, potassium hydroxide and hydrochloric acid were obtained from Fisher Scientific. Salicylaldehyde, sodium borohydride, 1, 1'-carbonyl-diimidazole and tris- (2-aminoethyl) amine (TREN) were obtained from Sigma Aldrich. Anhydrous ferric chloride

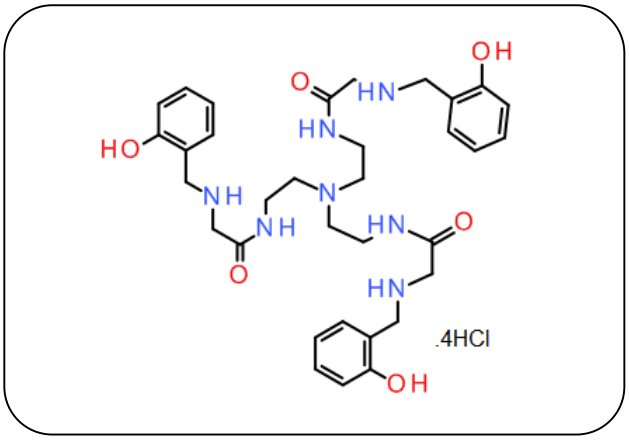

Fig. 2: Molecular structure of N-[2-[bis[2-[[2-[(2-hydroxyphenyl)methylamino] acetyl]amino] ethyl]amino] ethyl]-2-[(2-hydroxyphenyl)methylamino]acetamide (TRENglySAL).

was procured from Qualigens Fine Chemicals (Thermo Fisher Scientific) and solvents were brought from Merck. Chemicals were used as purchased without further purification. Solvents were dried using standard methods [14].

Melting points (mp) were determined on a Microsil (India) MP apparatus and are uncorrected. They are expressed in degree centigrade (°C). Infrared (IR) spectra were recorded on a Perkin-Elmer RX 1 FT-IR spectrometer using KBr disc. NMR spectra were recorded on a Bruker Avance II 400 NMR spectrometer at SAIF Panjab University Chandigarh using tetramethylsilane (TMS) as an internal reference. The chemical shifts are expressed in parts per million (ppm). The mass spectrum was performed on Waters Micromass Q-TOF Micro with electron spray ionization (EI) technique at SAIF Panjab University Chandigarh. C, H, N analysis was carried out on EURO EA elemental analyzer with model EURO EA 3000.

Synthesis of N-[2-[bis[2-[[2-[(2-hydroxyphenyl)methylamino]acetyl]amino]ethyl]amino] ethyl]-2-[(2hydroxyphenyl)methylamino]acetamide (TRENglySAL)

N-(2-hydroxybenzyl)glycine (glysal) was synthesized adopting a literature procedure and was characterized. A solution of glycine (6.0g, 80mmol) and potassium hydroxide (4.5g, 80mmol) in 40 ml of water was added to 20 mL of an ethanolic solution of salicylaldehyde (9.6g, 80 mmol). The reaction mixture was kept on stirring for 2 hours. A dark yellow solution was obtained, to which one equivalent of sodium borohydride (3.0g, 80mmol) and 5-6 drops of a saturated aqueous solution of sodium hydroxide was added dropwise. The solution became white and turbid; it was stirred for another twelve hours. Subsequently, the solution was filtered off and the pH was adjusted to 4 with concentrated hydrochloric acid. On refrigeration, a white solid was obtained, which was collected by filtration, washed with ethanol and dried in vacuum. To the suspension of glysal (3.55 g, 19.6mmol) in 10 mL of THF, 1,1'-carbonyldiimidazole (3.17 g, 19.6 mmol) was added in 1:1 molar ratio. The mixture was refluxed for three hours. TREN (0.95 g, 0.0065mmol) in 20 ml of THF was added dropwise for a period of one hour at reflux. A gummy pale orange product was obtained. The product was dissolved with a minimum amount of water and then acidified with HCl to yield a white precipitate which was filtered and vacuum dried. Melting point 120° C, Yield= 54 %. IR (KBr pellet, cm^{-1}) 3423 , 3150 ,1693 , 1643 , 1560 , 855 , 752 , 717 ; ^{1}H NMR (D_2O/DCl , δ ppm) 6.93, (d, J=8.12, 3H, Ar-H), 7.01, (t, J=11.32, 3H, Ar-H), 7.22, (d, J=7.48, 3H, Ar-H),7.37, (t, J= 14.4, 3H, Ar-H), 4.47, (t, J= 4.4, 6H, $-CH_2$), 4.07, (t, J=10.32, 6H, $-CH_2$), 7.701, (s, 2H, $-NH_2^+$), 3.00 (t. J=12.48, 6H , $-CH_2$) , 3.76 (t, J=4.64, $-CH_2$) ; ^{13}C NMR (D_2O/DCl , δ ppm) 167.80 , 155.31 , 150.32 , 140.20, 129.60 , 123.95 , 118.90 , 49.54 , 47.78 , 46.34 , 45.71; Mass spectrum molecular ion peak m/z = 779.3. , Anal. Calcd. $C_{33}H_{45}N_7O_6$.4HCl C= 50.36 (50.71 calc.), H= 6.69 (6.39 calc.) and N= 12.94 (12.57 calc.).

Titration procedure

The potentiometric studies of the ligand and metal complexes were carried out by maintaining the temperature 25 ± 1°C using a double-wall glass jacketed titration cell connected to a constant temperature circulatory bath. Glass electrode coupled with Sension-02 pH meter was used to perform the titration. Calibration of the instrument was done by the standard method using buffer solutions. Titrations were carried out between the standard solution of HCl and KOH and the pH meter reading was converted to hydrogen ion concentration by using calculated hydrogen ion concentration (pK_w =13.77 ± .05).

Triple distilled, deoxygenated and deionized water was used for the preparation of all the solutions. Standardization of the 0.1 M solution of KOH was done against potassium hydrogen phthalate. HCl solution

(0.1M) was prepared and standardized against previously standardized KOH solution. 0.1 M ionic strength was maintained by adding calculated amount of 1 M KCl solution. Due to the low solubility of the ligand in water, 0.01 M solution of the ligand was prepared in 0.1 M HCl solution; and 0.01 M metal ion solution was prepared by using anhydrous ferric chloride in water. The final concentration of the ligand and metal were maintained to 0.001 M. Initial total volume of the titration mixture was 50 mL. The pH meter reading was taken after each addition of the base and sufficient time was allowed to acquire the equilibrium. Computer program HYPERQUAD 2006 [15] was used to determine the protonation constants of ligand and formation constants of Fe (III) complexes. Program HySS [16] was employed for obtaining the pH-dependent species distribution diagram from the measured equilibrium constant.

Spectrophotometric titrations were carried out under the same conditions as for potentiometric titrations. In these studies, a dilute solution of ligands (1×10^{-5} M) and a metal ion (1×10^{-5} M) was made acidic by adding the appropriate amount of 0.1M HCl at an ionic strength of 0.1M KCl and titrated against standard 0.1M KOH solution. After each addition of the base sufficient time was given to attain the equilibrium. When a constant value of pH was attained, then an aliquot of the solution was taken out to take the spectra. Transfer of the solutions was done very carefully to minimize the error due to volume loss. Computer program pHAb was used to determine the protonation constants of ligand and formation constants of Fe (III) complexes.

Molecular Modeling

All calculations were performed using a window based computer program Cache version 6.11, Hyperchem 7.5 and Spartan 10. The machine used was Pentium (R) IV having windows XP environment 3.20 GHz CPU. The minimum strain geometry of the ligand and the proposed metal complex were obtained initially by applying molecular mechanics methods and MM^+ force field and re-optimized using semi-empirical PM3 method in Hyperchem version 7.5. The conformational search was carried out using Spartan 10 and the minimum energy conformational structure was used for further calculation. The electronic spectra of the ligand, HOMOs, and LUMOs corresponding to the experimentally obtained peaks were calculated using optimized structure by applying ZINDO using INDO/1 parameters. The infrared spectrum was calculated with MOPAC using PM3 parameters. The spectra obtained theoretically are compared with that of the experimental ones.

RESULTS AND DISCUSSION

Synthesis of TRENglySAL

The reduced Schiff base of glycine and salicylaldehyde (glysal) was synthesized using the method adopted by *Gorkum et al.,* [17] with certain modifications (Scheme 1). The condensation product was not isolable as such; however, a white crystalline solid could be isolated after the reduction *in situ* followed by acidifying the solution with conc. HCl. Prior to condensation of glysal with TREN, the carboxylic group was activated by 1,1'-carbonyldiimidazole, which has higher selectivity in activating the carboxylic group than an o-hydroxyl group of the aromatic ring [18]. A voluminous white solid of imidazolide acid was formed, condensed with TREN to give a pale orange product (Scheme 1). The product was filtered, dissolved in water and upon acidification with HCl white solid TRENglySAL was obtained. To explore the reason for the low yield (50%), the filtrate of the pale orange product was evaporated on a rotary evaporator. A colorless liquid soluble in THF was obtained, TLC of which was different from the reactants and TRENglySAL. The formation could be due to activation of some hydroxyl group of glysal to some extent. Synthesis of the ligand was also attempted in which salt of glycine ester was used and the binding site was made free by neutralizing with a base TEA followed by the condensation with salicylaldehyde in ethanol medium. A dark yellow solution was obtained which was then condensed to TREN giving an orange liquid. Attempts to isolate the solid product were unsuccessful.

Characterization of TRENglySAL

IR spectrum of the ligand TRENglySAL (Fig. 3a) recorded as KBr pellet, showed the absence of a broad peak at 3330-3500 cm^{-1} for the $–NH_2$ group of the TREN. The disappearance of the peak at 3121 cm^{-1} of the –OH group of carboxylic acid group of glysal indicates the condensation of glysal and TREN. A broad peak at 3423 cm^{-1} was observed due to ν (-NH) of amide, ν (-NH) of amine and ν (-OH). The appearance of the peaks

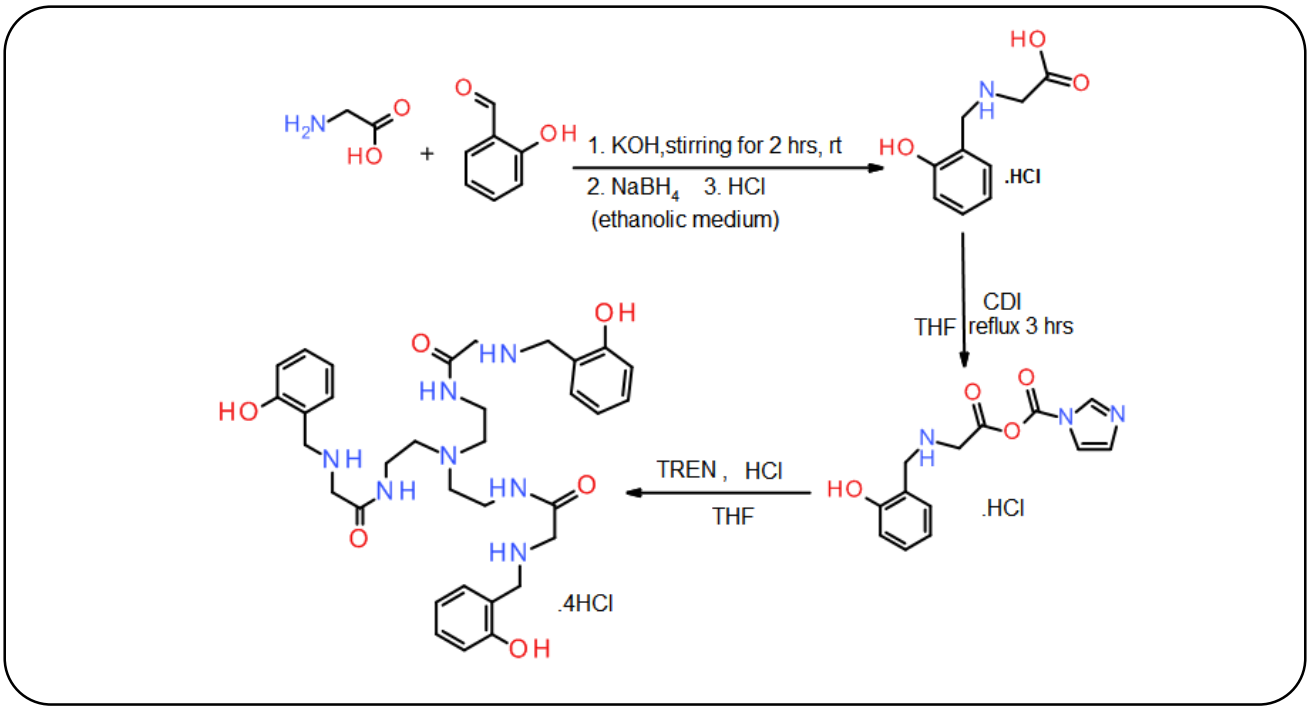

Scheme 1: Synthesis of TRENglySAL.

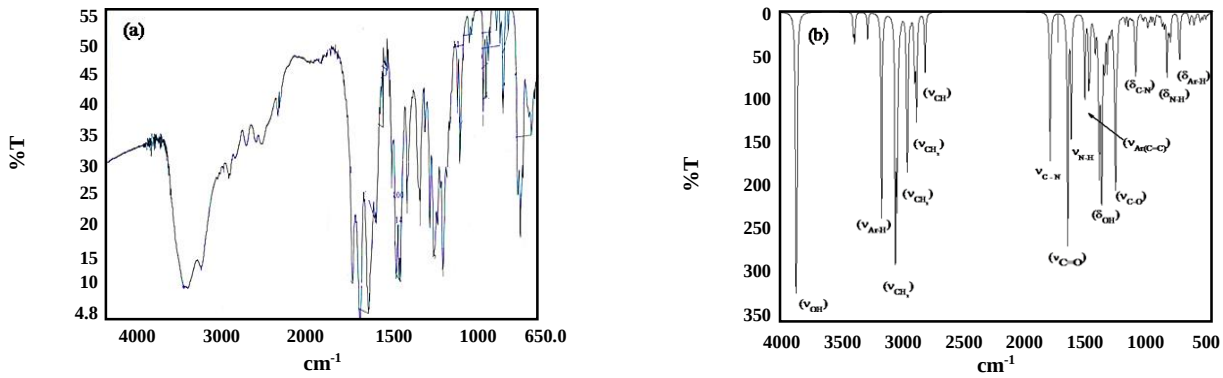

Fig. 3: (a) Experimental IR spectrum of TRENglySAL (KBr pellet, cm^{-1}) (b) Theoretical IR spectrum of TRENglySAL calculated using semi-empirical PM3 methods

at 1693 cm^{-1} and 1560 cm^{-1} can be assigned to –C=O stretching and –NH bending of the amide group. Interaction of -C-N stretching band with -N-H bending mode gives rise to two new bands which can be assigned to the peaks obtained at 1737 cm^{-1} and 1554 cm^{-1}, respectively. Presence of amine linkage can be confirmed by the appearance of the peaks at 1643 cm^{-1} for -N-H in-plane bending and 855 cm^{-1} for -N-H wagging. Characteristic sharp peak for =C-H (out of plane) bending mode is obtained at 752 cm^{-1}. The IR spectrum of the ligand was also calculated theoretically by semi-empirical method (PM3). The trend of the theoretically calculated peaks matched with the experimental peaks. Linear correlation is found between experimental and theoretical IR data with an acceptable correlation coefficient R^2=0.9943 (Fig. 4).

The electronic spectrum of TRENglySAL (10^{-5}M), recorded in an aqueous medium is shown in Fig. 5a. Two bands at 218 and 275 nm were observed due to $\pi \rightarrow \pi^*$ transitions of the phenyl ring. The electronic spectrum

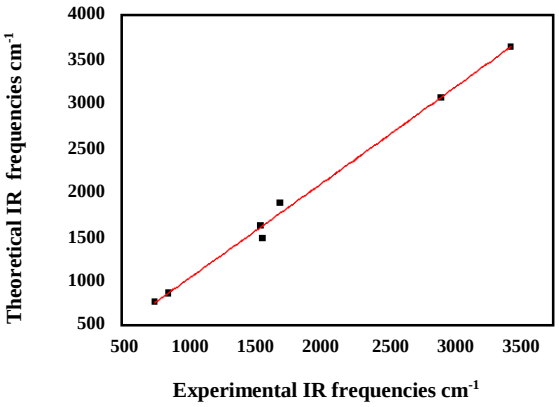

Fig. 4: Correlation between experimental and calculated IR frequencies of TRENglySAL.

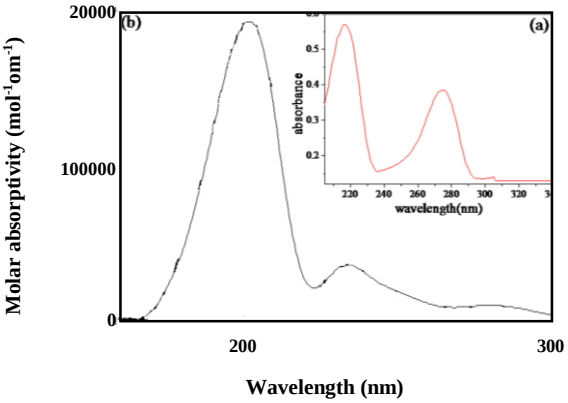

Fig. 5: a) Experimental electronic spectrum of TRENglySAL in aqueous solution (10^{-5} M) (b) Theoretical electronic spectrum of TRENglySAL calculated by applying ZINDO using INDO/1 parameters after optimizing geometry with MOPAC PM3.

calculated theoretically also showed two peaks at 200 nm and 235 nm (Fig. 5b). The absorption maxima obtained theoretically corroborated with the experimental one. The absorption intensity for both the peaks also affirms well with that of the experimental result. The HOMO and LUMO of the corresponding bands are shown in Fig. 6. It is clear that the HOMO and LUMO for the peaks are associated with the phenyl rings. The assignments are further confirmed by comparing the bands obtained for phenol that are usually observed at 210 nm and 275 nm for primary and secondary transition bands due to $\pi \rightarrow \pi^*$ transitions.

The structure of the ligand is also confirmed through ^{1}H NMR spectroscopy (Fig. 7). Two triplets were obtained at 4.47 ppm (6H) and 4.07 ppm (6H), assigned to aliphatic protons. The higher value corresponds to the hydrogens of the carbon attached to the phenyl ring. Peaks at 6.95 ppm (3H, doublet), 7.01 ppm (3H, triplet), 7.23 ppm (3H, doublet), 7.37 ppm (3H, triplet) correspond to the presence of aromatic protons. A broad singlet is obtained at 7.87 ppm (6H) may be for the amine protons ($>NH_2^+$ Cl^-). Two triplets obtained at 3.00 ppm (6H) and 3.76 ppm (6H) is for the protons of the aliphatic carbons of TREN which got deshielded due to the presence of amide linkage nearby.

The mass spectrum of the ligand, shown in Fig. 8 showed the molecular ion peak for TRENglySAL ($C_{33}H_{45}N_7O_6$).4HCl at 779.3(20%) (th: 779.24). The base peak at 213.1(100%) corresponds to the fragment $C_9H_{10}N_2O_2$.HCl, that may be formed due to the breaking of the bond of nitrogen of amide linkage and carbon of methylene group. A peak at 162.1 (70%) is found to fit with the formulation $C_9H_{10}N_2O$, which may be due to the removal of -OH, HCl and two protons from the base peak fragment. The suggested fragmentation pattern is shown in Fig. 9. The formulation of the compound is also confirmed through C, H, N analysis, C= 50.36 (50.71% calc.), H= 6.69% (6.39% calc.) and N= 12.94 (12.57% calc.).

Ligand protonation constant

The formation of metal complexes is viewed as a competition between the protons of ligand moiety and metal ions. Hence, the protonation constants of the ligand were evaluated experimentally, which are required as input data for calculation the formation constants of the metal complexes. The potentiometric titration of the ligand, TRENglySAL, was carried out in presence of an excess measured amount of 0.1 M HCl against 0.1M KOH in aqueous solution at a constant ionic strength of 0.1M KCl and 25 ±1°C. The titration curves are shown in Fig. 10. "a" on x-axis corresponds to moles of base added per mole of ligand present and y-axis to pH of the reaction cell. The titrations are performed within the pH range 2-12. After the neutralization of the excess added acid, the dissociation of the protons occurs in steps between pH 4-10.5. Analysis of the potentiometric titration curves using the program HYPERQUAD 2006 gave best fit for seven protonation constants (Table 1). The following equation depicts the protonation reaction:

$$LH_{n-1} + H \rightleftarrows LH_n,\ K_n = [LH_n]/[LH_{n-1}][H] \quad (I)$$

where, n=1, 2, 3, 4, 5, 6, 7

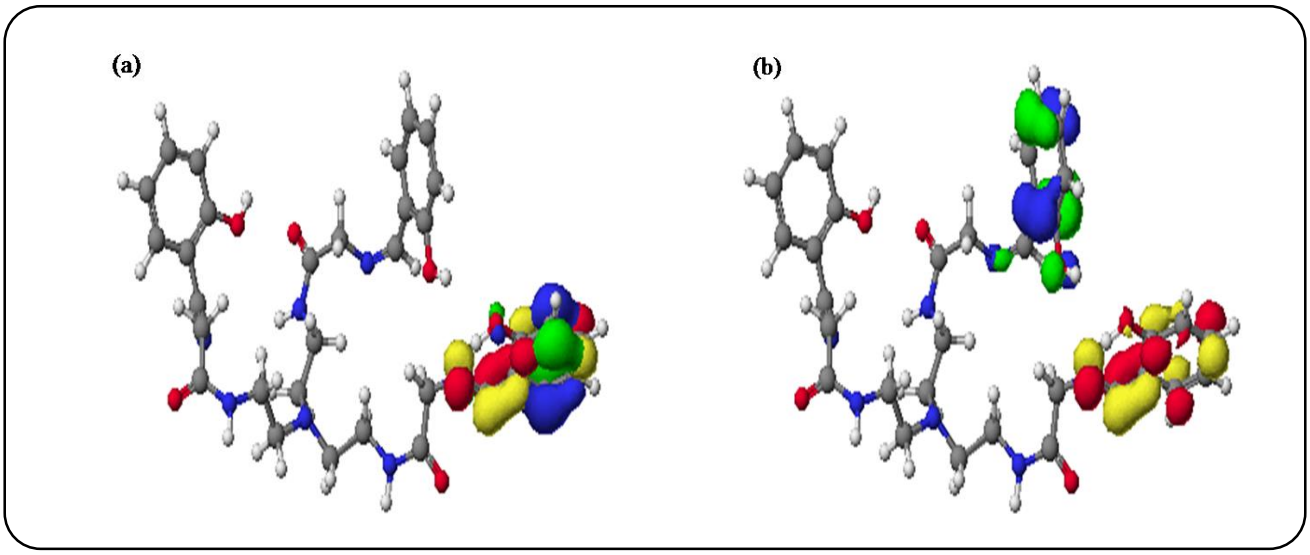

Fig. 6: HOMO and LUMO diagrams for TRENglySAL corresponding to the peaks (a) at 200 and (b) at 235 nm, calculated by applying ZINDO using INDO/1 parameters after optimizing geometry with MOPAC PM3

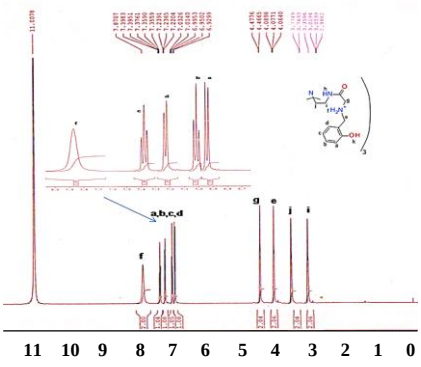

Fig. 7: ^{1}H NMR spectrum of TRENglySAL in $CDCl_3$ / DCl.

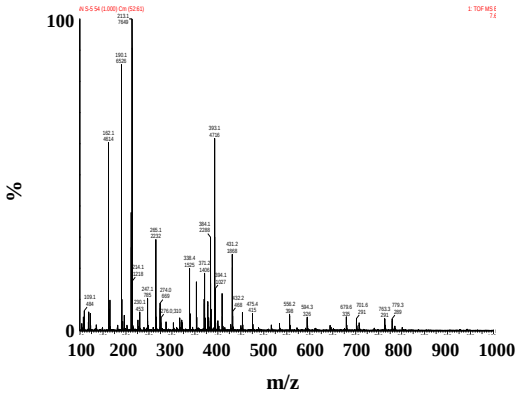

Fig. 8: Mass spectrum of TRENglySAL by MS(ES+).

The protonated secondary amine of glycine moiety, capping tertiary amine and phenol are supposed to undergo deprotonation giving overall seven protonation constants (Table 1). The basic amine protons deprotonate comparatively at higher (i.e., pH > 9) than the phenolic protons (pH =4-7). The ligand is assumed as tri-protic acid LH_3; but, in its fully protonated form, it is assumed to be $(LH_7)^{4+}$. The values of protonation constants for the phenolic protons are found to be lower than phenol (pKa ~ 10); this indicates the presence of intramolecular hydrogen bonding. Molecular modeling study also reveals the presence of intramolecular hydrogen bonding between the phenolic protons with the secondary amine as well as with the amide nitrogen of neighboring arm (Fig. 11).

Protonation constants of the ligand were also determined by spectrophotometric method. In this method a pH versus absorbance measurement was carried out at ligand concentration (1×10^{-5} M), 25 ± 1^0 C and constant ionic strength 0.1M KCl. The absorbance spectra of the ligand were recorded within the pH range 3-11 and are shown in Fig. 12a. No appreciable change in the electronic spectra was observed below experimental pH 4.13 and above pH 10.43. The equilibrium between various protonated and deprotonated species was examined from the spectral changes like shifting of peaks and formation of isosbestic points. The whole range of spectral data (as shown in Fig. 12a) by non-linear least square fitting program pHAb gave best fit for only three protonation constants.

Table 1: Protonation constants of the ligand, TRENglySAL (T= 25 ± 1^0 C, μ=0.1 M KCl) A (Potentiometry), B (Spectrophotometry).

Species	Equilibrium		Log K	
			A	B
	$L^{3-} + H^+ \rightleftarrows HL^{2-}$	N_s-H	11.29	-
	$HL^{2-} + H^+ \rightleftarrows H_2L^{1-}$	N_s-H	10.68	-
	$H_2L^{1-} + H^+ \rightleftarrows H_3L$	N_s-H	9.89	-
	$H_3L + H^+ \rightleftarrows H_4L^+$	O-H	8.62	8.60
	$H_4L^+ + H^+ \rightleftarrows H_5L^{2+}$	O-H	7.81	7.81
	$H_5L^{2+} + H^+ \rightleftarrows H_6L^{3+}$	O-H	6.61	6.63
	$H_6L^{3+} + H^+ \rightleftarrows H_7L^{4+}$	N_t-H	5.79	-

(N_s- secondary amine, O- phenolic OH, N_t- tertiary amine)

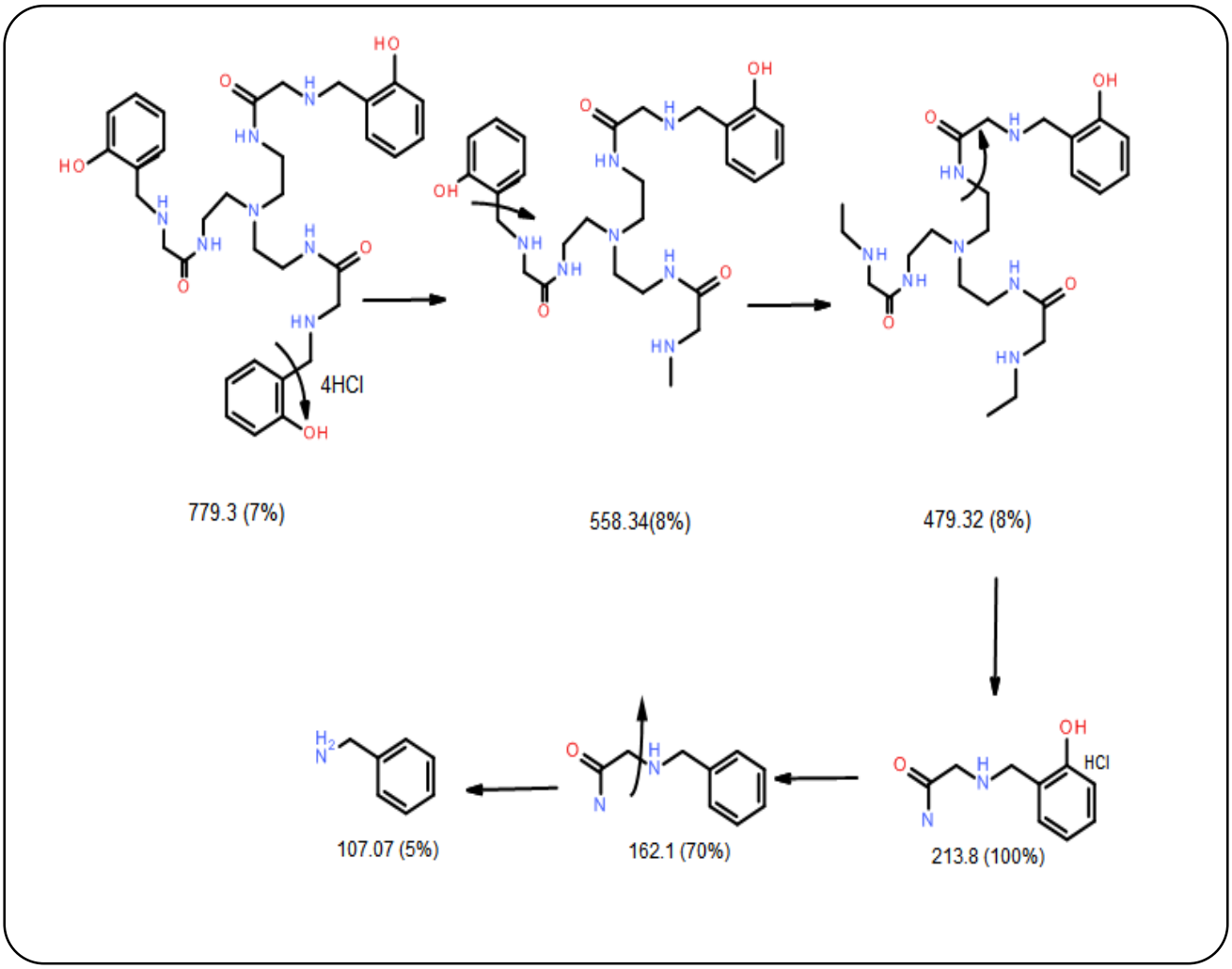

Fig. 9: Suggested fragmentation pattern of TRENglySAL.

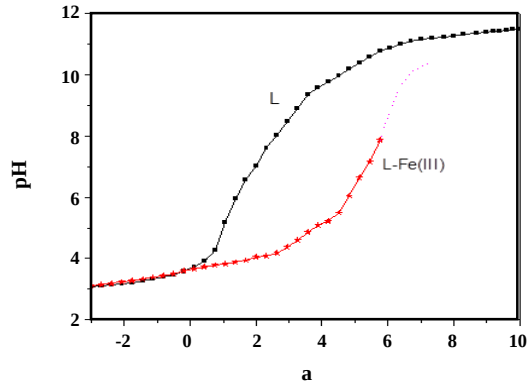

Fig. 10: Potentiometric titration curves: 1× 10^{-3} M [TRENglySAL] (L), 1× 10^{-3} M [Fe(III)], [L-Fe(III] in 1:1 molar ratio, T= 25 ± 1^0 C , 0.1 M KCl and 'a' is the moles of base added per mole of ligand/complex.

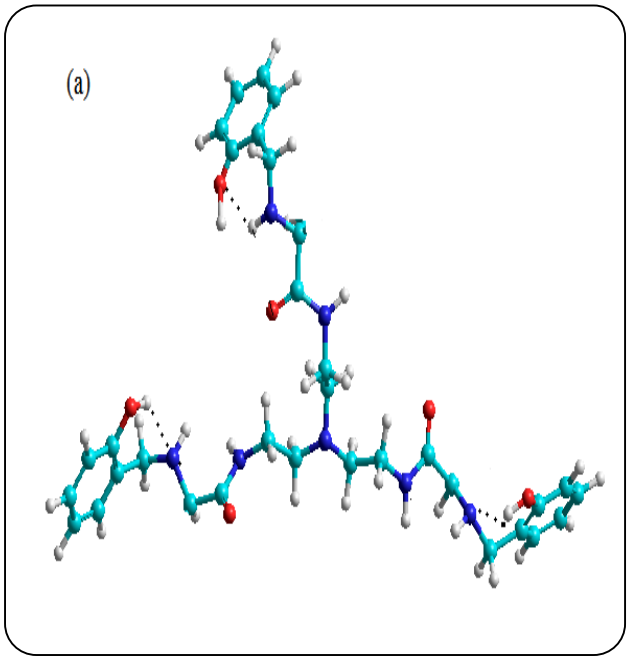

Fig. 11: Least strain energy structure of the TRENglySAL calculated by using semi-empirical PM3 method

Both the electronic spectral maxima of 218 nm and 275 nm that obtained earlier, showed bathochromic and hyperchromic shift with increasing pH. They appeared at 235 nm and 295 nm. The shifting of the peaks to longer wavelength can be explained by the fact that on deprotonation, formation of phenolate ion takes place which stabilizes the π^* excited state due to charge delocalization and brings the lowest excited closer to the highest ground state, and thus permits a lower energy (longer wavelength) for the transition. It may be noted that, seven protonation constants were evaluated by the potentiometric method, however, only three protonation constants could be obtained by a spectrophotometric method. This variation may be attributed to the presence of the only chromophoric phenol group in the ligand responsible for the spectral deviations. The first three protonation constants (logK); 11.29, 10.68 and 9.89 are ascribed to a secondary amine, and values 8.62, 7.81 and 6.61 are attributed to phenolic protons of the ligand. These types of assignments for tripodal aminophenolate ligands are also documented [19]. The lowest protonation constant logK= 5.79 is assigned to the capping tertiary amine nitrogen of TREN backbone as in TRENCAM (logK=5.88) and TRENglyCAM (logK=5.89).

The pH-dependent species distribution diagram of the ligand, obtained from their calculated protonation constants is shown in Fig. 13a. The diagram shows that at the initial stage ligand exists 100% in its fully protonated form $[LH_7]^{4+}$ below pH 5. Stepwise deprotonation of the ligand occurs with the formation of $[LH_6]^{3+}$, $[LH_5]^{2+}$, $[LH_4]^{1+}$, LH_3, $[LH_2]^{1-}$, $[LH]^{2-}$ and $[L]^{3-}$ species with the increase of pH from 5 to 11. The highest percentage of formation for LH_3 is 80%. At pH ~ 10.0, the complete deprotonation starts and the fully deprotonated form of the ligand L^{3-} becomes predominant after pH 11.

The protonation constants of the ligand were compared with some structurally similar tripodal ligands. Table 2 displays the protonation constant values of TRENglySAL, TRNS, TAMS, TAPS, TACS [19] TRENCAT [20], THAC [21], TMACHCAT [8], TRENGlyCAM [11] and their parent tripodal ligand TMACH [22], TREN [23], TACH [24], TAME [25] and TAP [26] for the comparison. The first three values of protonation constants are alike to TMACHCAT, TRENCAT, and TRNS and are attributed due to the deprotonation of –NH- group. For TAPS, TAS and TAMS pKa_3 is different, which is assigned to –OH group. Orvig *et al.*, had reported earlier that if the central amine has a pKa < 8 then this pKa decreases in amine phenol but if pKa > 8 in the central amine system then pKa increases in the corresponding amine phenol. On the other hand, if pKa < 8 in the parent amine, then the secondary amine group will deprotonate first and, if pKa > 8 then phenol group will deprotonate first in the amine phenol system. This is also true for TRENglySAL. Here, the deprotonation starts from the phenolic group followed

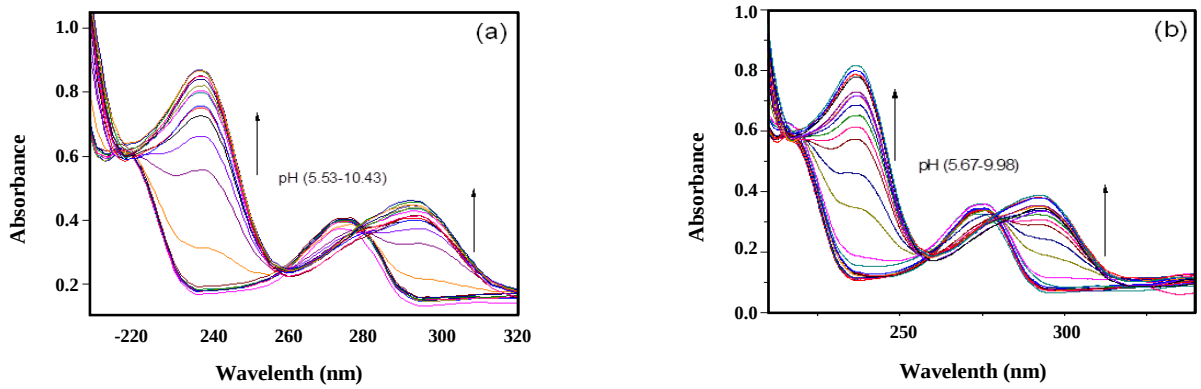

Fig. 12: pH dependent electronic spectra as a function of absorbance and wavelength for (a) TRENglySAL and (b) 1:1 solution of Fe(III) and TRENglySAL, [TRENglySAL] = [Fe(III)] = 1× 10^{-5} M, T= 25 ± 1^0 C, 0.1 M KCl.

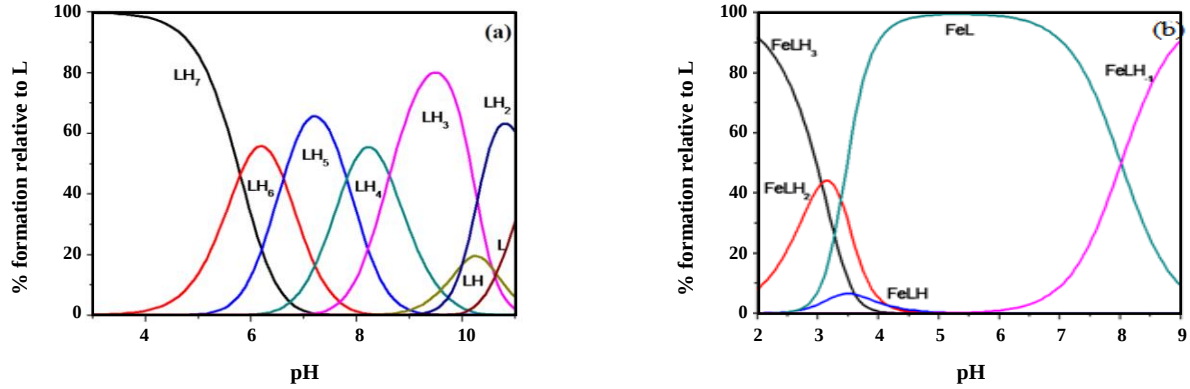

Fig. 13: Species distribution curves computed from the (a) protonation constants for TRENglySAL and (b) formation constants for Fe(TRENglySAL), [TRENglySAL]$_{tot}$ = [Fe(III)]$_{tot}$ = 10^{-5} M, solvent: water, T= 25 ± 1^0 C at 0.1 M KCl.

by the secondary amine groups. For TRNS, the apical nitrogen is known to be very acidic (pKa < 1.5) because of the possibility of four nitrogen atoms sharing the three hydrogen atoms through hydrogen bonds. However, in TRENglySAL, due to amide linkage, the hydrogens are in tautomeric forms and are not available for hydrogen bonding with the apical nitrogen. Hence, the lowest protonation constant value is assigned to the apical nitrogen as in the case of TRENGlyCAM.

To check the authentication of the assigned protonation constants, gas phase free energy change of the proposed species was calculated by semi-empirical PM3 quantum mechanical method. Dissociation of an acid AH can be represented by the reaction AH = A^- + H^+. Free energy change and pK_a are related by the thermodynamic relation pKa = $\Delta G_{gas,AH}$ / 2.303 RT. For the dissociation reaction of AH, the gas phase free energy is obtained according to the following equation:

$\Delta G_{gas,AH}$ = (G_{gas,A^-} + G_{gas,H^+}) - $G_{gas,AH}$, Proton free energy at 298 K and 1atm is;

G_{gas,H^+} = 2.5 RT - T ΔS^o = 1.48 - 7.76 = -6.28 kcal/mol [27]

ΔG value must decrease during a deprotonation process. A clear decrease in ΔG values is observed for TRENglySAL as the protons deprotonate from secondary amine, tertiary amine, and phenolic groups. The values obtained theoretically are compared with the experimental pKa, which gave an acceptable correlation R^2 = 0.99073 (Fig. 14).

Complex formation with trivalent Fe (III) metal ion

Various species formed due to the interaction of TRENglySAL with Fe(III) ion have been probed at variable pH by the combined use of potentiometric and spectrophotometric titrations at 25±1°C in an

Table 2: TRENglySAL and other reported Tripodal ligands and their protonation constants [21] (logK) (A- Potentiometry and B-Spectrophotometry).

	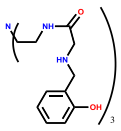 TRENglySAL		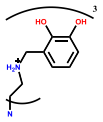 TRENCAT	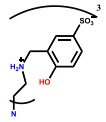 TRNS	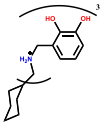 TMACHCAT	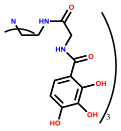 TRENGlyCAM		
Assignments	A	B	A	A	A	B	A	
N-H	11.29	-	11.23	11.2	11.26	11.2	12.9	
N-H	10.68	-	10.61	10.6	10.65	1	12.1	
N-H	9.89	-	9.75	9.59	9.80	10.6	11.3	
O-H	8.62	8.60	8.51	8.07	8.48	5	8.33	
O-H	7.81	7.81	7.58	7.29	7.61	9.79	7.54	
O-H	6.61	6.63	6.32	6.17	6.23	8.47	6.84	
N_t–H	5.79	-			-	7.60	5.89	
						6.22		
						-		

	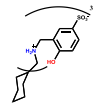 TACS	 TAMS	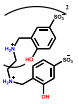 TAPS	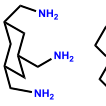 TMACH	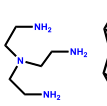 TREN	 TACH	 TAME	 TAP	
Assignments	A	A	A	A	A	A	A	A	
N-H	11.24	11.19	11.24	10.53	10.13	10.16	10.16	9.64	
N-H	9.84	9.81	9.77	9.84	9.43	8.66	8.25	7.89	
O-H	8.59	8.91	8.73	-	-	-	-	-	
O-H	7.85	7.95	7.78	-	-	-	-	-	
O-H	7.08	6.56	6.54	-	-	-	-	-	
N-H	6.01	2.92	1.7	8.88	8.41	7.17	5.85	3.72	

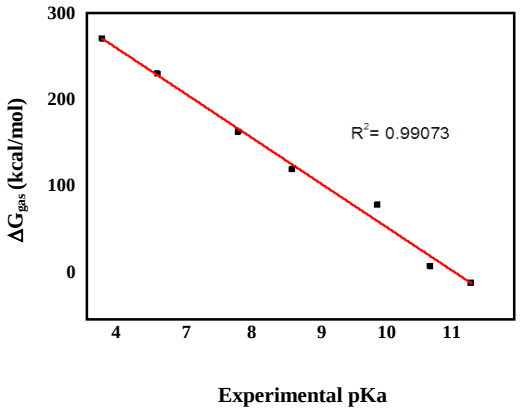

Fig. 14: Correlation between the experimental log K and calculated gas phase free energy change of various deprotonated species formed in solution for the ligand TRENglySAL.

aqueous solution. The potentiometric titration curves of 1:1 solution of ligand (0.001M) and Fe(III) (0.001M) is shown in Fig. 10. The curve for the metal-ligand complex deviates considerably from the curve of the free ligand with a variation in pH indicating the release of proton upon metal coordination and formation of the complex. The nature of curves qualitatively indicates that the ligand has a prominent affinity to the metal ion. The inflection of the curve at a = 6 indicates the formation of species in which six protons have been displaced from TRENglySAL by Fe(III). Further, the increase in pH led the formation of hydroxo-complex which could be indicated by the formation of turbidity. A number of models were tested to refine the potentiometric data by Hyperquad 2006 program, but, the best one involves the formation

Table 3: Spectral Overall (logβ) for the Fe (III) metal complexes formed by the TRENglySAL (T= 25 ± 1⁰ C, μ=0.1 M KCl).

Species	Equilibrium	Fe(III) (Log β)	
		A	B
$FeLH_3$	$Fe^{3+} + L^{3-} + 3[H]^{+} \rightleftarrows [FeLH_3]^{3+}$	35.15	35.16
$FeLH_2$	$Fe^{3+} + L^{3-} + 2[H]^{+} \rightleftarrows [FeLH_2]^{2+}$	32.09	32.08
FeLH	$Fe^{3+} + L^{3-} + [H]^{1+} \rightleftarrows [FeLH]^{1+}$	27.91	27.91
FeL	$Fe^{3+} + L^{3-} \rightleftarrows [FeL]$	25.32	25.31
$FeLH_{-1}$	$Fe^{3+} + L^{3-} + [H]^{1-} \rightleftarrows FeLH_{-1}$	17.32	17.33

A (Potentiometry), B (Spectrophotometry)

of the species MLH_3, MLH_2, MLH, ML, and MLH_{-1}. The overall formation constants (log β) of the species are reported in Table 3.

The equilibrium reactions for the complex species formed and their formation constants, β_{11n} , can be described by the following equations (where L-Ligand, M- Fe (III) metal ion, H- Hydrogen, n= 1, 2, 3,-1):

$M + L \rightleftarrows ML \qquad \beta_{110} = [ML]/[M][L]$ II

$M + L + H \rightleftarrows MLH \qquad \beta_{111}=[MLH]/[M][L][H]$ III

$M + L + 2H \rightleftarrows MLH_2 \qquad \beta_{112} = [MLH_2]/[M][L][H]^2$ IV

$M + L + 3H \rightleftarrows MLH_3$ V

$\beta_{113} = [MLH_3]/[M][L][H]^3$

$M + L \rightleftarrows MLH_{-1} + H^{+}$ VI

$\beta_{11-1} = [MLH_{-1}][H^{+}]/[M][H]$

To authenticate the results of the potentiometric method, the spectrophotometric method was also employed to determine the formation constants. The spectrophotometric titrations were carried out in aqueous solution at ligand concentration (1×10^{-5} M) and metal ion concentration (1×10^{-5} M) at 25± 1^0 C and ionic strength 0.1 M KCl. The electronic spectra of ligand were recorded in the pH range 5.67-9.98 (Fig. 12b). Shifting of the peaks was observed along with the formation of isosbestic points as the pH was increased continuously. Peaks at 218 and 275 nm were shifted bathochromically to the wavelength 235 and 297 nm respectively. The appearance of the new peak at 235 nm is due to the hyperchromic shift of band at 218 nm. The low-intensity secondary band for phenyl ring also experienced an appreciable bathochromic and hyperchromic shift with increasing pH. These shifts, and appearance of the isosbestic points indicate the interaction of the metal ion with the ligand as the different species in equilibrium have different spectra. However, no additional band due to metal-ligand bond is observed. This may be due to the very low concentration of the solution. The similarity in the variations in the spectra of the metal-complex formation is due to ligand-proton complex formation. The global fitting of the spectral data in the program pHab resulted in five formation constants as obtained in the potentiometric method. The results are compiled in Table 3.

The species distribution curves for the ligand in presence of metal ion clearly illuminate the complex formation of the ligand with the metal ion (Fig. 13b). The formation of the complex started at pH ~ 2.5 with the formation of MLH_3 . With the increase in pH, the following MLH_2, MLH, ML, and MLH_{-1} species are formed successively. Phenolic oxygens are expected to coordinate first to the metal ion. Amine nitrogen tends to coordinate later due to their higher basicity. At initial stages, Fe (III) is considered as a hexa-aqua complex. As the pH increases the water molecule are replaced with the phenolic oxygen and later with the amine nitrogen to form the N_3O_3 octahedral complex. The previous report of *Orvig et. al.* [19] on the coordination behaviour of similar tripodal aminophenolate ligands suggest that, such monomeric ML complexes exist in solution as a mixture of species: one in which the ligand coordinated through N_3O_3 sets, and second, the $ML(H_2O)$, where the ligand binds metal ion through N_3O_2 or N_2O_3 donor sets and one water molecule coordinated to the central metal ion to complete the octahedron. Subsequently, the coordinated water molecule releases a proton to give hydrolyzed species. Similar coordination modes are also noticed in the complexes of THAC, an aminophenolate ligand. But,

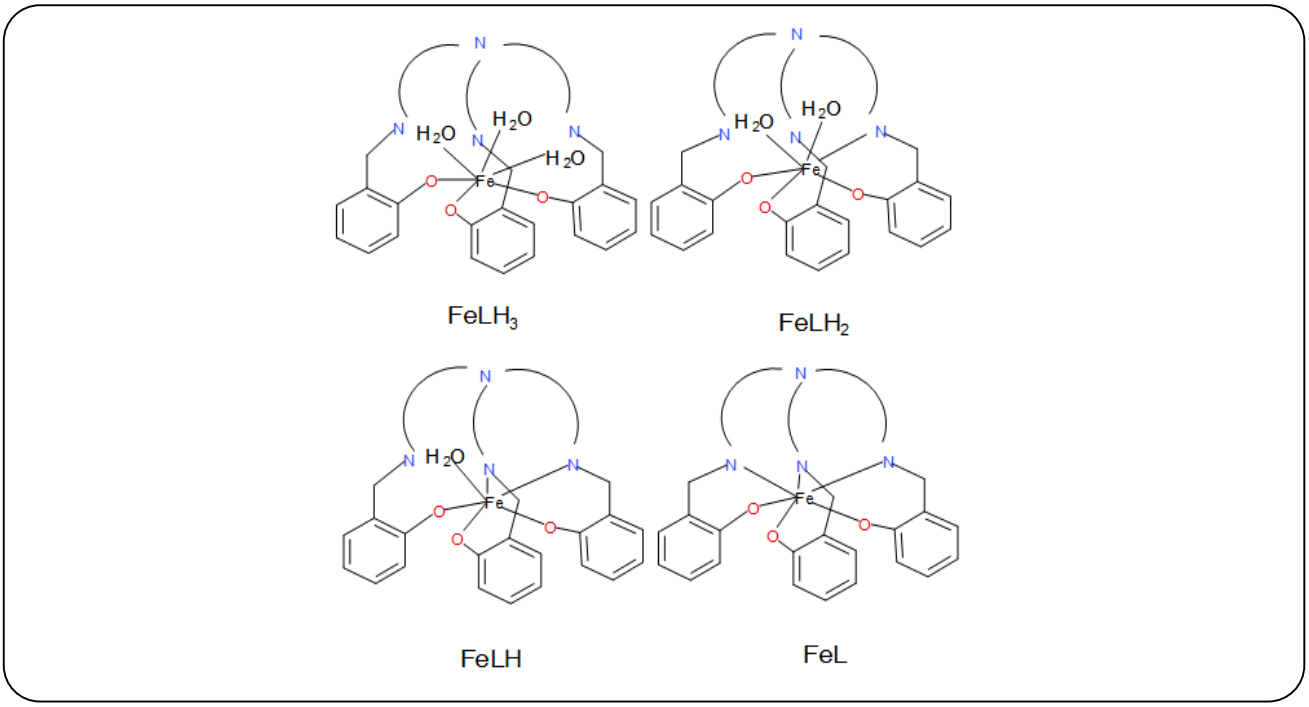

Fig. 15: Coordination modes in [Fe(III)-TRENglySAL] complex in 1:1 molar ratio.

in the present case, coordination through N_3O_2 donor sets is ruled out as the bathochromic shifting of the peak was observed in a higher pH indicating coordination of phenolate. Also, the Fe^{3+}, being a hard metal ion has a higher preference for the phenolate oxygen than nitrogen of the amine. Based on these observations, it can be suggested that the ligand can form two types of ML complexes: ML, in which coordination donor sets is N_3O_3, and $ML(H_2O)$ through N_2O_3. For the ligand THAC, all the phenolic protons were deprotonated below pH 8, whereas in case of TRENglySAL, the experimental pH is raised up to 11 for which it can be assumed that complete deprotonation of phenolic and amide protons occur ruling out of N_3O_2type of coordination. It can be summarized that on interaction of the ligand with the metal ion, a number of species are formed as function of pH, the predominant one among them is ML species that exists in pH range from ~3 to ~9 indicating the ligand opts to form 1:1 metal complex by coordinating through N_3O_3 donor sites. Structures of various species formed during complexation are proposed in Fig. 15. Energy minimized structure and some physical structural parameters of the ML type complex calculated are given in Fig. 16 and Table 4 respectively. The geometry of the metal complexes is predicted through theoretical calculations as distorted octahedral.

ΔH_f = (heat of formation), E_T = (total energy)

The complexing ability of the ligand to a metal ion under specific environmental condition can be expressed as pM, which is defined as $-\log[M(H_2O)_n]^{m+}$, and can be calculated using pH-dependent stability constants at physiological pH=7.4, taking $[L]=10^{-5}$ M and $[M]=10^{-6}$M. A higher pM value (low concentration of uncomplexed metal ion) indicates a more stable complex formation. If pM value is below Ksp of $Fe(OH)_3$, that leads the precipitation of the hydroxide. The calculated pM value of the ligand for Fe3+ ion at pH 7.4 along with the literature pM values of some ligand related ligands of biological importance are given in Table 5. A higher pM value in Fe(III)-TRENglysal system confirms the higher ligand's binding efficacy towards the metal ion. Comparison of the result of Table 5 shows that the pFe value of TRENglySAL is lower as compared to the ligands containing catecholate binding moiety. This difference may be explained considering HSAB principle, where Fe(III) is a hard acid, hence it prefers oxygen as a coordination site on priority rather than nitrogen. On the contrary, when compared with other similar ligands (containing salicylate) like TMACHSAL and Me_3TMACHSAL, the values are found to be higher. The extended flexibility to the molecular structure to the

Table 4: Some calculated parameters for the metal complex, [Fe-TRENglySAL](1:1) by using the semi-empirical PM3 method.

Bond length(A^0)		Bond angle(^{0})			ΔH_f (Kcal/mol)	E_T (eV)
Fe-O	Fe-N	N-Fe-O	N-Fe-N	O-Fe-O		
1.84	1.95					
1.83	1.94	94	93.2	92.8	-16.93	-6143.92
1.84	1.91					

Table 5: Comparison of pFe values of TRENglySAL with some chelators reported.

Salicylate Ligands	pFe	Catecholate ligands	pFe	Other chelators	pFe
TRENglySAL	23.86	MECAM	29.1	Transferrin	20.3
TMACHSAL	20.14	TRENCAM	27.8	DMHP	19.3
Me_3TMACHSAL	16.41	TRENGlyCAM	30.9	Defriprone	19.6
		TRENAlaCAM	28.0		
		TRENGluCAM	30.9		

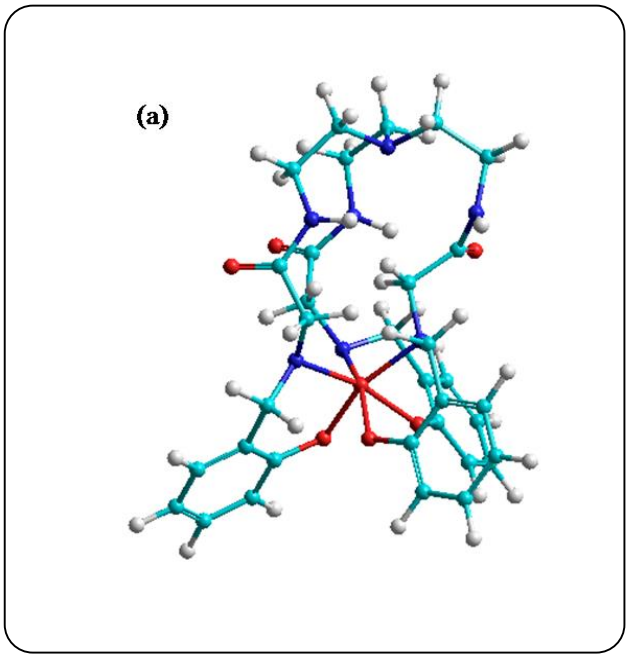

Fig. 16: The calculated structure of [Fe(III)-TRENglySAL] using semi-empirical PM6 method.

pendant arms may be one of the reasons for the extra stability. The podant also exhibits higher pFe values as compared to Transferrin and Deferiprone.

CONCLUSIONS

This paper describes the synthesis and iron binding capability of a new tripodal ligand that mimicks the natural siderophore bacillibactin, (an excellent binder with iron) by changing the coordination sites from O_3O_3 instead of N_3O_3. The complexation behavior of the tripodal chelator, TRENglySAL was explored in an aqueous medium by adopting both potentiometric and spectrophotometric methods. Seven protonation constants were determined, which can be assigned to the tertiary amine of TREN (central unit), secondary amine of glycine (spacer) and a phenolic group of salicylaldehyde (binding unit). The formation constants (log β) of the Fe(III) complexes with the ligand were determined. Formation of species viz., MLH_3, MLH_2, MLH, ML, MLH_{-1} occur in different pH range. The high formation constant values indicate an outstanding affinity of the ligand towards Fe(III) metal ion and renders as more potent iron chelator at physiological pH. Greater flexibility in the pendant arms and the presence of hydrogen bonds in the tripod provides an additional stabilization allow the desired octahedral arrangement to be less strained. Among the various species formed, ML is the most stable existing over a large pH range 3-9 as is a single major species at biological pH. Theoretical studies supported the preference of ML species formation with higher stability inferring a N_3O_3 hexadentate coordination modes showing slightly distorted octahedral geometry. The high binding affinity of the ligand towards Fe(III) metal ion can be exploited further towards its utilization for the removal of Fe(III) in iron overload chelation therapy. Also, the noticeable

electronic spectral changes of the complex with the pH variant support the ligand for a potential optical sensor towards Fe(III) metal ion in biological systems.

Acknowledgments

The authors would like to thank Council of Scientific and Industrial Research (CSIR), Human Resource Development Group, PUSA, New Delhi, India for financial Support, also to National Institute of Technology, Kurukshetra, Haryana, India for providing infrastructure and research facilities.

Received : Nov. 10, 2019 ; Accepted : Jan. 18, 2019

REFERENCES

[1] d'Hardemare A.D.M., Alnaga N., Serratrice G., Pierre J.L., Oxinobactin, a Siderophore Analogue to Enterobactin Involving 8-Hydroxyquinoline Subunits: Synthesis and Iron Binding Ability, *Bioorg. Med. Chem. Lett.*, **18**: 6476-6478 (2008).

[2] Abergel R.J., Zawadzka A.M., Hoette T.M., Raymonds K.N., Enzymatic Hydrolysis of Trilactone Siderophores: Where Chiral Recognition Occurs in Enterobactin and Bacillibactin Iron Transport(1), *J. Am. Chem. Soc.*, **131**: 12682-12692 (2009).

[3] Isied S.S., Kuo G., Raymond K.N., Coordination Isomers of Biological Iron Transport Compounds. V. The Preparation and Chirality of the Chromium(III) Enterobactin Complex and Model Tris(catechol) Chromium(III) Analogues, *J. Am. Chem. Soc.*, **98**: 1763-1767 (1976).

[4] O'Brien I.G., Gibson F., The Structure of Enterochelin and Related 2,3-dihydroxy-N-benzoyne Conjugates from Eschericha Coli, *Biochimica et Biophysica Acta*, **215**: 393-402 (1970).

[5] Pollack J.R., Nielands J.B., Enterobactin, an Iron Transport Compound from Salmonella Typhimurium, *Biochem. Biophys. Res. Commun*., **38**: 989-992 (1970).

[6] Moerlein S.M., Welch M.J., Raymond K.N., Weitle F.L., Tricatecholamide Analogs of Enterobactin as Gallium- and Indium-Binding Radiopharmaceuticals, *J. Nuc. Med.*, **22**: 710-719 (1981).

[7] Tor Y., Libman J., Shanzer A., Felder C.E., Lifson S., Tripodal Peptides with Chiral Conformations Stabilized by Interstrand Hydrogen Bonds, *J. Am. Chem.l Soc.*, **114**: 6653-6661 (1992).

[8] Imbert D., Thomas F., Baret P., Serratrice G., Gaude D., Pierre J.L., Laulhere J.P., Synthesis and Iron(III) Complexing Ability of CacCAM, a New Analog of Enterobactin Possessing a Free Carboxylic Anchor arm. Comparative Studies with TRENCAM, *New J. Chem.*, **24**: 281-288 (2000).

[9] Piyamongkal S., Zhou T., Liu Z.D., Khodr H.H., Hider R.C., Design and Characterisation of Novel Hexadentate 3-hydroxypyridin-4-one Ligands, *Tetrahedron Letters*, **46**: 1333-1336 (2005).

[10] Baral M., Sahoo S. K., Kanungo B. K., Tripodal Amine Catechol Ligands: A Fascinating Class of Chelators for Aluminium(III), *J. Inorg. Biochem.*, **102**: 1581-1588 (2008).

[11] Dertz E.A., Xu J., Raymond K.N., Tren-based Analogs of Bacillibactin: Structure and Stability, *Inorg. Chem.*, **45**: 5465-5478 (2006).

[12] Evans D.F., Jakubovic D.A., Water-Soluble Hexadentate Schiff-Base Ligands as Sequestrating Agents for Iron(III) and Gallium(III), *J. Chem. Soc. Dalton Transactions*, **56**: 2927-2933 (1988).

[13] Evans D.F., Jakubovic D. A., Complexes of a Water-soluble tridentate schiff base Ligand with a Number of "Hard" Metal Ions, *Polyhedron*, **7**: 1881- (1988).

[14] Furniss B.S., Hannaford A.J., G.Smith P.W., Tatchell A.R., "Vogel's Textbook of Practical Organic Chemistry", Dorling Kindersley, India (2009).

[15] Gans P., Sabatini A., Vacca A., Investigation of Equilibria in Solution. Determination of Euilibrium Constants with the HYPERQUAD Suite of Programs, *Talanta*, **43**: 1739-1753 (1996).

[16] Alderighi L., Gans P., Lenco A., Peters D., Sabatini A., Vacca A., Hyperquad Simulation and Speciation (HySS): a Uility Program for the Investigation of Equilibria Involving Soluble and Partially Soluble Species, *Coord. Chem. Rev.*, **184**: 311-318 (1999).

[17] Gorkum R.V., Berding J., Tooke D.M., Spek A.L., Reedijk J., Bowman E., The Autoxidation Activity of New Mixed-Ligand Manganese and Iron Complexes with Tripodal Ligands, *J. of Cat.*, **252**: 110-118 (2007).

[18] Staab, H. A., "New Methods of Preparative Organic Chmistry IV. Syntheses Using Heterocyclic Amides", Angewandte Chemie International Edition in English, 1, 351 (1962).

[19] Caravan P. Orgiv C., Tripodal Aminophenolate Ligand Complexes of Aluminum(III), Gallium(III), and Indium(III) in Water, *Inorg. Chem.*, **36**: 236-248 (1997).

[20] Bismondo A., Comuzzi C., Di Bernardo P., Luigi Zanonato P., Complexation of Thorium(IV) by Tris((2,3-dihydroxybenzylamino)ethyl)amine—A New Strong Chelating Agent, *Inorganica Chimica Acta*, **286**(1): 103–107 (1999).

[21] Sahoo S.K., Baral M., Kanungo B.K., Potentiometric, Spectrophotometric, Theoretical Studies and Binding Properties of a Novel Tripodal Polycatechol-Amine Ligand with Lanthanide (III) Ions, *Polyhedron*, **25**: 722-736 (2006);
Sahoo S.K., Baral M., Kanungo B.K., Potentiometric and Spectrophotometric Studies on the Binding Ability of a Flexible Tripodal Catecholamine Ligand Towards Iron(III), *J. Chem. Eng. Data*, **56**: 2849-2855 (2011);
Sahoo S.K., Bera R.K., Kanungo B.K., Baral M., Spectroscopic and pH-Metric Studies on the Complexation of a Novel Tripodal Amine-Phenol Ligand Towards Al(III), Ga(III) and In(III), *Spectrochimica Acta Part A*, **89**: 322-328 (2012).

[22] Muthu S. E., "Studies on Metal Complexes of some Multidentate and Macrocyclic Ligands", Ph.D Thesis, Punjab Technical University, India (2004).

[23] Martell A.E., Smith R.M., "Critical Stability Constants", Vols. 1-6, Plenum, New York (1974).

[24] Childers R.F., Wentworth R.A.D., Zompa L.J., Potentiometric and Spectrophotometric Studies on the Binding Ability of a Flexible Tripodal Catecholamine Ligand Towards Iron(III), *Inorg. Chem.*, **10**: 302-306 (1971).

[25] Micheloni M., Sabatini A., Vacca A., Nickel(II), Copper(II) and Zinc(II) Complexes of 1,1,1-Tris(Aminomethyl)Propane. a Calculation Procedure of Stepwise Formation Constants and Their Standard Errors from The Values Obtained for the Cumulative Equilibria, *Inorg. Chim. Acta*., **25**: 41-48 (1977).

[26] Cini R., Giorgi G., Masi D., Sabatini A., Vacca A., Synthesis and Crystal Structure of Propane-1,2,3-Triamine Trihydrochloride Monohydrate. Reactions of Propane-1,2,3-Triamine with Hydrogen Ion. Thermodynamic Functions and Molecular Mechanics Calculations , *J. Chem. Soc. Perkin Trans.*, **2**: 765-771 (1991).

[27] Topol I.A., Tawa G.J., Burt S.K., Rashin A.A., On the Structure and Thermodynamics of Solvated Monoatomic Ions Using a Hybrid Solvation Model, *J. Chem. Phy.*, **111**: 10998 (1999).